Digital holography with ultimate sensitivity

M. Gross and M. Atlan

Laboratoire Kastler-Brossel de l'École Normale Supérieure,
CNRS UMR 8552 - Université Pierre et Marie Curie,
24 rue Lhomond 75231 Paris cedex 05. France

We propose a variant of the heterodyne holography scheme, which combines the properties of off-axis and phase-shifting holography. This scheme makes it possible filter-off numerically the zero order image alias, and the technical noise of the reference. It is then possible to record and reconstruct holographic images at an extremely low signal level. We show experimentally that the sensitivity of the method is limited only by the quantum nature of photons.

Digital holography is a fast-growing research field that has drawn increasing attention [1]. The main advantage of digital holography is that, contrarily to holography with photographic plates [2], the holograms are recorded by a CCD and the image is digitally reconstructed by a computer, avoiding photographic processing [3]. Off-axis holography [4] is the oldest and the simplest configuration adapted to digital holography [5, 6, 7].

In off-axis digital holography, as well as in photographic plates holography, the reference or local oscillator (LO) beam is angularly tilted with respect to the object observation axis. It is then possible to record, with a single hologram, the two quadratures of the object complex field. However, the object field of view is reduced, since one must avoid the overlapping of the image with the conjugate image alias [8].

Phase shifting digital holography [9, 10] records several images with different phase for the LO beam. It is then possible to obtain the two quadratures of the field in an on axis configuration even though the conjugate image alias and the true image overlap, because aliases can be removed by taking images differences.

In this paper, we propose a digital holography technique that combines off-axis geometry (introduced by Schnars et al. [6]), with the use of a sequence of images obtained with different phase shifts of the LO beam to record the hologram in amplitude and phase (as proposed by Yamaguchi et al. [9]). To get precise phase shift, Le Clerc's et al. [10] heterodyne technique is used. Using a spatial filtering method (Cuche's et al. [8]), the zero order image, and the noise attached to it, is filtered-off numerically. As shown experimentally, this combination of techniques makes it possible to record and reconstruct holographic images at a very low level of signal: 1 photo electron of signal per reconstructed image pixel during a whole sequence of 12 images ($\simeq$ 1 s). This corresponds to the ultimate quantum limit.

The setup is shown on Fig.1. It is similar to the one used in [10, 11]. The main laser L is a Sanyo DL-7140-201 diode laser ($\lambda = 785$ nm, 50 mW for 95 mA of current). It is split into an illumination beam (frequency ω_L, complex field E_L), and in a LO beam (ω_{LO}, E_{LO}). The object we want to image is an USAF target in transmission, which is back illuminated. The object signal
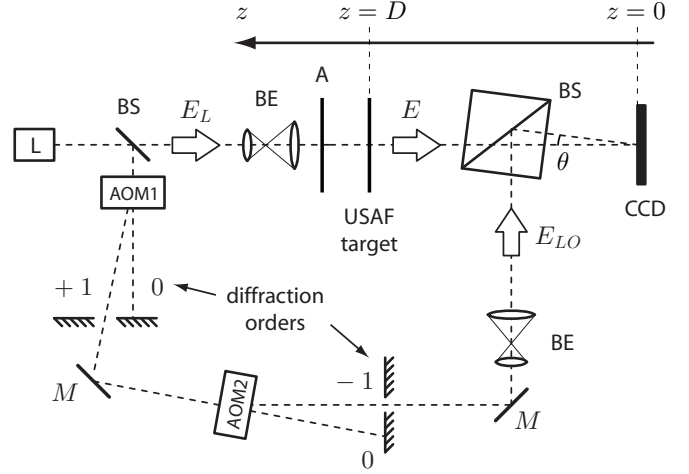

FIG. 1: USAF target digital holography setup. L: main laser; BS: Beam splitter; AOM1 and AOM2: acousto optic modulators; BE: beam expander; M: mirror; A: light attenuator. USAF: transmission USAF target. CCD : CCD camera.

field E is not shifted in frequency (ω_L). A set of optical attenuators A (grey neutral filter) is used to reduce the illumination. The CCD camera (PCO Pixelfly digital camera: 12 bit, frame rate $\omega_{CCD} = 12.5$ Hz, acquisition time $T = 1/12.5 = 80$ ms, with 1280×1024 pixels of $6.7 \times 6.7\,\mu$m) records the hologram of the object, i.e. the object (E) and LO (E_{LO}) field interference pattern. Using AOM1 and AOM2 acousto optic modulators (Crystal Technology: $\omega_{AOM1,2} \simeq 80$ MHz), the optical frequency ω_{LO} of the LO beam, can be freely adjusted. To make 4-phases detection of the object field E, the LO frequency is adjusted to be $\omega_{LO} = \omega_L + \omega_{CCD}/4$ [10]. Moreover the LO beam is tilted (angle $\theta \sim 1°$) with respect to the camera to object observation axis. Our holographic setup thus works both in off-axis and in phase shifting mode.

A sequence of 12 CCD images I_0 to I_{11} (measurement time 0.96 s) is recorded. Since the LO beam is phase shifted by $\pi/2$ between two consecutive images, the object complex hologram H is obtained by summing the

CCD images with the appropriate phase shift:

$$H = \sum_{m=0}^{11} (j)^m I_m \qquad (1)$$

where m is the image index and $j^2 = -1$.

We have reconstruct the images of the USAF target by using the standard convolution method [6, 12] that yields a calculation grid equal to the pixel size. To calculate the convolution product, we have used the Fourier method, like in [10]. To make faster Fourier calculation the 1028×1024 CCD data are truncated to a 1024×1024 2D matrix.

The reconstruction algorithm is the following. The real space hologram $H(x, y, z)$ in the $z = 0$ CCD plane is calculated by Eq.1. The hologram in the CCD reciprocal plane (i.e. in the $z = 0$ k-space) is obtained by Fourier transformation:

$$\tilde{H}(k_x, k_y, 0) = FFT [H(x, y, 0)] \qquad (2)$$

The k-space hologram at any distance z from the CCD is then:

$$\tilde{H}(k_x, k_y, z) = \tilde{K}(k_x, k_y, z) \tilde{H}(k_x, k_y, z) \qquad (3)$$

where $\tilde{K}$ is the k-space kernel function that describe the propagation from 0 to z.

$$\tilde{K}(k_x, k_y, z) = e^{jz(k_x{}^2 + k_y{}^2)/k} \qquad (4)$$

where $k = 2\pi/\lambda$ is the optical wave vector. The reconstructed image, which is the hologram in the object plane ($z = D$), is then obtained by reverse Fourier transformation:

$$H(x, y, z) = FFT^{-1} \left[\tilde{H}(k_x, k_y, z) \right] \qquad (5)$$

Fig.2a shows the intensity of the CCD plane complex hologram (i.e. $|H(x, y, 0)|^2$). The USAF target is seen, but is blurred. Fig.2b shows the intensity of the CCD plane k-space hologram (i.e. $|H(k_x, k_y, 0)|^2$). The bright zone in the left hand side of the image corresponds to the true holographic image i.e. to the interference of the object field with the LO field. The zero-order and twin image [8] alias contributions are very low. The zero-order alias, in the center of the k-space hologram (pixel 512, 512), is weak, because the contribution of the LO intensity cancels out by making difference of images (Eq.1). Since the phase shift provided by the acousto optic modulators is very close to a multiple of $\pi/2$, the twin-image is also very weak. It is barely not visible on Fig.2b, although the display is in grey logarithmic scale.

To select the relevant first order image information, and to fully suppress the zero-order and twin image aliases, we have used the k-space filtering method developed by Cuche et al. [8]. We have selected, in the k-space 1024×1024 matrix, a 200×200 region of interest centered on the true image bright zone. Note that this selection is made possible by the off-axis geometry that has
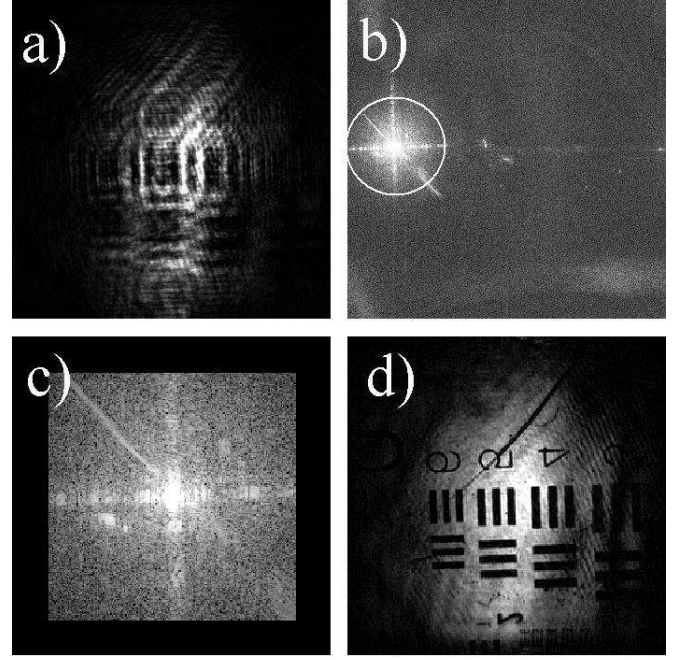

FIG. 2: Reconstruction of the USAF target image. (a) Intensity image of the CCD complex hologram $|H(x, y, 0)|^2$ in linear grey scale. (b) Intensity image of the k-space hologram $|\tilde{H}(k_x, k_y, 0)|^2$ in logarithmic grey scale. (c) Intensity image of the truncated k-space hologram in logarithmic grey scale. (d) USAF target reconstructed image, i.e. intensity image of the real space hologram in the object plane $|H(x, y, D)|^2$ in linear grey scale. Images are 1024×1024 (a,b), or in 256×256 (c,d) pixels.

translated the true image in the left hand side of k-space matrix. The selected area is then copied in the center of a 256×256 zero matrix (zero padding). The calculation of the $z = D$ k-space and real space holograms (Eq.3 and Eq.5) are thus done on this 256×256 calculation grid. Fig.2c shows the object plane k-space hologram (i.e. $\tilde{H}(k_x, k_y, z)$) in the 256×256 grid. Fig.2d shows the object plane real space hologram (i.e. $H(x, y, z)$) obtained by the Eq.5 reverse FFT, which is the reconstructed image of the USAF target. Note that the translation of the selected zone in the center of the k-space in Fig.2c moves the reconstructed USAF target to the center of the image as seen in Fig.2d.

We have assessed the sensitivity limit of this off-axis heterodyne holography technique by recording images of the USAF target at different levels of illumination. To get quantitative results, we have determined the absolute number of photo electrons that correspond to the signal beam. First, we have calibrated our set of attenuators (A) at the working wavelength (785 nm). These attenuators were then used to change the illumination of the USAF target while the laser power remained constant throughout the experiment. For a high level of illumination of the USAF target, and without LO beam, we have
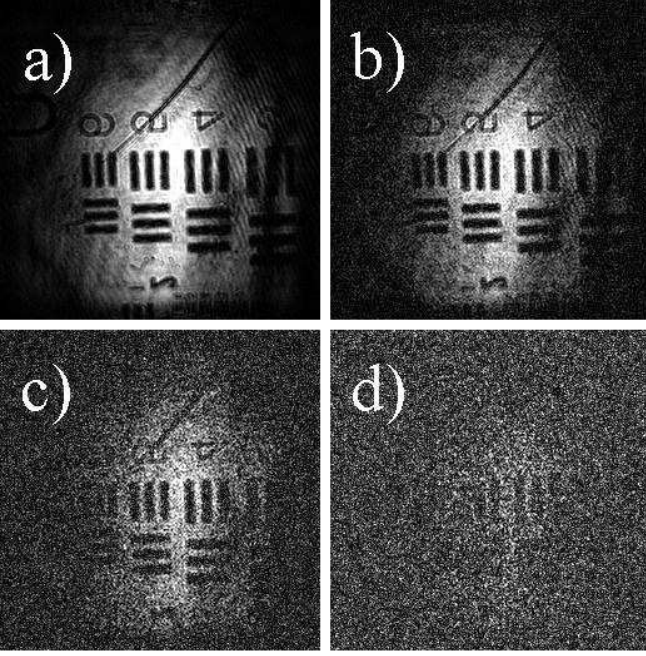
FIG. 3: Reconstructed image of a USAF target in transmission with low light illumination. Images are obtained with a signal field that corresponds to $\simeq 2.8 \times 10^7$ (a), 2.8×10^5 (b), 4×10^4 (c) and 6000 (d) photo electrons for the whole 12 CCD images (256×256 pixels displayed in linear grey scale).

measured the signal beam in photo electrons units: we have multiplied the CCD signal in digital counts (0...4095 DC) by the CCD gain ($G = 2.4$ photo electrons per DC: PCO calibration). For other levels of illumination (for a given set of attenuators in the object arm), we have calculated the signal beam level in photo electrons units, from the attenuators calibration.

Fig.3 shows the reconstructed images that are obtained at various levels of illumination. Figs.3 a to d are obtained with $\simeq 2.8 \times 10^7$ (a), 2.8×10^5 (b), 4×10^4 (c) and 6000 (d) photo electrons of signal for the whole set of 12 CCD images. It should be noticed that the total number of photo electron is not the relevant parameter to characterize the image signal. Since the reconstruction is performed with a truncation over a 200×200 pixels region of the k-space, the reconstructed image has about 4×10^4 resolved pixels. The signal can thus be characterized by the number of photo electrons per resolved pixel. Therefore, the images of Fig.3 correspond to 700 (a), 7 (b), 1 (c) and 0.15 (d) photo electrons per pixel. For comparison, the image of Fig.2d corresponds to 3.5×10^4 photo electrons per pixel.

One photo electron per resolved pixel is the quantum limit of visibility of an image (i.e. the limit that is related to the quantum character of photons, and photo electrons). Fig.3c image corresponds exactly to this limit, where the SNR of the image is about 1. This demonstrate that our off-axis heterodyne technique is able to

filter-off technical noise and to reach the quantum limit of photodetection. Note that it is still possible to perceive the USAF target on Fig.3d with only 0.15 photo electron per pixel (SNR$\simeq 0.15$).

This result can be understood quite simply. In the case of a very weak signal, the majority of the technical noise is within the LO beam (because the signal beam is much weaker than the LO beam). This noise can be eliminated by a double filtering process. First, most of the noise is removed by taking the difference of successive images (Eq.1). This is the phase-shifting filtering that occurs in the temporal frequency domain. But this method doesn't remove all the technical noise. Since the LO beam extends within a few spatial modes (i.e. a few pixels of the k-space), its noise is located near the center of the k-space. This means that the LO technical noise is flat field (it varies slowly in space). A spatial filtering similar to the one introduced by Cuche et al. [8] removes the rest of the technical noise which lies in the center of the k-space. This is the off-axis filtering that occurs in spatial frequency domain.

The digital holography technique presented here relies on the combination of off-axis and phase-shifting configurations to record holograms with ultimate sensitivity. This technique lets one filter-off the local oscillator technical noise and reach the quantum sensitivity limit. As demonstrated, we were able to make an image with a signal of one photoelectron per pixel during a sequence of 12 recorded camera frames. Although demonstrated in through transmission this technique is expected to work as well in reflection with diffusely scattering surface. It might be used to perform holography with at extremely low signal level, e.g. nano-object imaging... We have used a variant of this technique to detect the so called "tagged photons" in acousto-optic imaging [13], or the photons that are transmitted through the breast, in vivo [14]. With a high quantum efficiency camera, the technique could also be used to perform quantum optics tests (non classical photon statistics, squeezed states).

[1] U. and W.P.O. Jüptner. Digital recording and numerical reconstruction of holograms. *Meas. Sci. Technol.*, 13, 2002.

[2] D. Gabor. Microscopy by reconstructed wave-fronts. *Proc. Royal Soc. London A*, 197:454–487, 1949.

[3] J. W. Goodmann and R. W. Lawrence. Digital image formation from electronically detected holograms. *Appl. Phys. Lett.*, 11:77, 1967.

[4] E.N. Leith, J. Upatnieks, and K.A. Haines. *J. Opt. Soc. Am*, 55:981–986, 1965.

[5] U. Schnars and W. Jüptner. Direct recording of holograms by a CCD target and numerical reconstruction. *Appl. Opt.*, 33(2):179–181, 10 January 1994.

[6] U. Schnars. Direct phase determination in hologram interferometry with use of digitally recorded holograms. *JOSA A.*, 11:977, July 1994.

[7] T. M. Kreis, W. P. O. Juptner, and J. Geldmacher. Principles of digital holographic interferometry. *SPIE*, 3478:45, July 1988.

[8] E. Cuche, P. Marquet, and C. Depeursinge. spatial filtering for zero-order and twin-image elimination in digital off-axis holography. *Appl. Opt.*, 39(23):4070–4075, 10 August 2000.

[9] I. Yamaguchi and T. Zhang. Phase-shifting digital holography. *Optics Letters*, 18(1):31, 1997.

[10] F. LeClerc, L. Collot, and M. Gross. Numerical heterodyne holography using 2d photo-detector arrays. *Optics Letters*, 25:716, Mai 2000.

[11] F. LeClerc, L. Collot, and M. Gross. Synthetic-aperture experiment in visible with on-axis digital heterodyne holography. *Optics Letters*, 26, October 2001.

[12] T. Kreis. Digital holography for metrologic applications. *in Interferometry in Speckle Light, P. Jacquot and J.-M. Fournier, eds., Springer Verlag*, pages 205 – 212, 2000.

[13] M. Gross, P. Goy, and M. Al-Koussa. Shot-noise detection of ultrasound-tagged photons in ultrasound-modulated optical imaging. *Opt. Lett.*, 28(24):2482–2484, 15 December 2003.

[14] M. Gross, P. Goy, B. C. Forget, M. Atlan, F. Ramaz, A. C. Boccara, and A. K. Dunn. Heterodyne detection of multiply scattered monochromatic light with a multipixel detector. *Opt. Lett.*, 30, 2005.